Journal of Sound and Vibration (1998) **212**(4), 703–719

A NOTE ON THE CONVERGENCE OF THE DIRECT COLLOCATION BOUNDARY ELEMENT METHOD

P. JUHL

Department of Acoustic Technology, Building 352, *Technical University of Denmark, DK*-2800 *Lyngby, Denmark*

(*Received* 24 *September* 1996, *and in final form* 8 *December* 1997)

Convergence results for acoustic boundary element formulations have mainly been presented in the mathematical and numerical literature, and the results do not seem to be widely known among acoustic engineers. In this paper, an overview of some of the literature dealing with convergence of boundary element formulations is presented, and an intuitive account of the results is given. The convergence of an axisymmetric boundary element formulation is studied by using linear, quadratic or superparametric elements. It is demonstrated how the rate of convergence of these formulations is reduced for calculations involving bodies with edges (geometric singularities). Two methods for improving the rate of convergence are suggested and examined. First, elements modelling the singular behaviour of the sound field are used, and then a novel technique of replacing the mid-element node is presented. The latter approach is a generalization of the well-known quarter point technique in which the mid-element node is displaced better to model the singularity.

1. INTRODUCTION

Boundary element methods have long been established as an important technique for the numerical calculation of acoustic problems. In the earliest formulations, constant elements in which the geometry and the acoustic variables were assumed to be piecewise constant were used [1]. Later, quadratic elements were introduced, either in order to obtain better accuracy [2] or to ensure compatibility with finite element methods [3], where quadratic elements are commonly used. It is well accepted among engineers that the use of the more advanced quadratic elements gives more accurate results than using constant or linear elements, but the theoretical results regarding accuracy and convergence of boundary element methods in other engineering areas do not seem to be well known in the acoustic community. In finite element theory, error analysis is more common, and may be found in standard textbooks, but convergence issues are not commented on in the dominant textbook for the boundary element methods in acoustics [4].

The paper is organized as follows. The remainder of this introduction contains comments on some of the work done on convergence of boundary element formulations in acoustics and other areas, with a focus on convergence for smooth objects and objects with corners, which is one of the topics investigated in this paper. Section 2 introduces some concepts relating to convergence, by using the classical example of numerical integration of a known function. Then the same line of thought is used to obtain convergence estimates for an axisymmetric boundary formulation—the direct collocation method based on the Helmholtz integral equation. It should be emphasized that although the convergence properties for simple numerical integration formulas can actually be found

0022–460X/98/190703 + 17 $25.00/0/sv971456

by expanding the function to be integrated into its Taylor series as indicated in section 2, the development in section 5 is not a rigorous mathematical analysis of convergence of the formulation under consideration. Such a rigorous mathematical analysis of the convergence of a number of boundary element formulations has been presented by Wendland [5]. The analysis of Wendland makes use of advanced functional analysis, and the results do not appear to be well known among acousticians and engineers.

The Helmholtz integral equation relates the pressure outside a closed body to a surface integral of the normal velocity and the pressure multiplied by respectively the Green function and its normal derivative with respect to the surface (plus—for scattering problems—an incoming wave). If a Neumann boundary condition is specified (i.e., if the surface velocity is known, which is the most common case) the equation is a Fredholm integral equation of the second kind, and convergence results can be found in reference [5]. The proof of the existence and convergence of the various boundary element formulations presented by Wendland (including the Helmholtz integral equation considered here) relies on the fact that the operators involved are strongly elliptic pseudo-differential operators. For these operators, one obtains optimal convergence in the energy norm for any *Galerkin scheme*, which means that the convergence rate is entirely determined by the question of how well the solution is approximated by the elements [6]. The Galerkin scheme is a variational approach in which the error made on the surface by introducing the shape functions is minimized over the entire surface, which means that for this method an additional integration over the surface of the object is carried out. This extra integration is avoided in the collocation method, where the integral equation is required to be satisfied only at certain points—collocation points. Since it is simpler and faster, the collocation technique is the most-used method for the standard case. Situations exist for which the variational approach is advantageous, but this is beyond the scope of this paper. Unfortunately, convergence proofs are more difficult for the collocation technique, but some results for the Helmholtz integral equation have been established in reference [5]. (For two dimensions, the collocation technique may be regarded as a modified Galerkin method for which convergence results are more easily found [5].) The error due to numerical integration of the kernel(s) and the error due to geometric discretization were included in Wendland's analysis by using the first Strang lemma [5], so convergence results are presented for the fully discretized versions of the integral equations. The discretization error and the quadrature error were also investigated in reference [7]. The convergence results mentioned above are valid for the so-called h version of the boundary element method. In convergence analysis it is customary to denote the typical element dimension by h, so the accuracy is investigated for diminishing mesh size; i.e., in the limit of $h \to 0$. In the h version of the method the order of the shape functions is kept constant. The general finding is that for the h version a power convergence rate is obtained; i.e., the error is reduced as h^m for $h \to 0$, where m is the convergence rate (the order of the shape functions plus one for optimal convergence) [5]. Hence, for linear elements, the expected convergence rate is two.

Another strategy for improving accuracy is the so-called p version. In the p version of the method the mesh is kept at a relatively coarse level, and accuracy is then improved by increasing the order of the shape functions. If the solution is sufficiently smooth (i.e., if the object is without edges and corners, which will be discussed later) the p version converges exponentially. This method has been investigated in acoustics in a formulation based on the Burton and Miller approach [8] and by using a Garlerkin scheme [9, 10]. In the paper of Geng *et al*. [10], it was proved that the operator of the Burton and Miller formulation is strongly elliptic, and hence the results of Wendland, Stephan and others outlined above could readily be used, and in the paper of Grannell *et al*. [9] numerical results were presented that (for the test cases considered) confirm the exponential decay of errors for scattering of smooth objects. The *p* version is expected to be best suited for the Galerkin approach, since the collocation points of a point collocation scheme would be too closely spaced for higher order elements [9]. It should be mentioned that the *p* version is not available with most commercial software, since it needs programming of the higher order elements in the code, whereas the *h* method is available with any BEM package in which the mesh is controlled by the user.

As indicated above, the convergence rate might be dependent on the smoothness of the true solution. One case in which an impedance jump generates a singularity in the true solution was investigated by Filippi [11], where special shape functions designed to model the nature of the singularity were used to resolve the singularity and improve the accuracy. This strategy of modelling the singularity with the shape functions was also suggested by Wendland [5], and originates from the FEM. A more prominent example of an acoustic singularity is the thin screen, which has been treated by various authors [12–15]. The knife edge scattering problem is the acoustic equivalent of the stress near a crack tip in an elastic body. In reference [12], the singularity was modelled by using singular shape functions, and in references [13–15] the quarter-point technique was adopted from the finite element method [16] to model the singularity.

The singular behaviour of an acoustic field near a corner of a rigid obstacle asymptotically resembles that of a field governed by Laplace's equation. For Laplace's equation subject to a Dirichlet boundary condition which leads to a Fredholm integral equation of the first kind, both the Galerkin method and the collocation point method were examined theoretically by Ervin and Stephan [17], and it was found that for uniform meshes the convergence rate was determined by the strength of the singularity, which was also mentioned by Rank [18]. Ervin and Stephan suggested to retain high accuracy by the use of exponentially graded meshes towards the singularity; i.e., an *h* version. In a later paper by Stephan [19], this approach was extended to Neumann problems for the Laplacian in three dimensions by using the Galerkin scheme (i.e., also the second kind Fredholm equation), and among others the *hp* version was reviewed. The idea of the *hp* version is to use a graded mesh with low order elements near the singularity (*h* version) and high order elements away from the singularities (*p* version), and it was found that the exponential convergence of the *p* version could be regained. For the Helmholtz integral equation, the *hp* version has been used for screen problems (which involve the knife edge) in two indirect Galerkin version boundary element formulations; namely, the single layer potential method for Dirichlet problems, and the normal derivative of the double layer potential method (i.e., the hypersingular kernel, which also appears in the Burton and Miller formulation) for Neumann problems [20]. Normally the *h*, *p* and *hp* versions are implemented adaptively; i.e., the program automatically decides to grade the mesh or to use higher order shape functions depending on an error estimate [18]. Error estimation for the Galerkin implementation of the Burton and Miller formulation in acoustics was carried out by Geng *et al*. [10], where the influence of a corner on the error estimator was also investigated, but no attempt to model the singular behaviour was made.

The purpose of the present paper is twofold. The first objective of this paper is to present the theory of convergence for acoustic engineers. This is done in two ways. First, an overview of the theory presented in the mathematical and numerical literature has been given in this section. This theory is recondite, and does not seem to be well known among acoustic engineers. Secondly, sections 2–5 give a simple introduction to, and a discussion of, convergence of the collocation boundary element method with the weight put on a more intuitive understanding of the phenomena involved. In section 5, test cases are presented to illustrate the findings. An empirical error analysis for the boundary element method on

Laplace's equation has been reported [21], but the reduction of the rate of convergence due to geometrical singularities was not present in the test cases presented there. The second objective of this paper is to advocate for the novel technique termed the generalized quarter point technique, which can be used along with existing boundary element codes, and improves the accuracy considerably for the problems considered.

2. CONVERGENCE OF REGULAR NUMERICAL INTEGRATION FORMULAS AND THE CONCEPT OF ORDER

For regular numerical integration, i.e., the numerical evaluation of the integral of a known function over a given interval, the convergence of different formulations is well investigated, and the results may be found in standard textbooks (see, e.g., that of Press *et al*. [22]). In this section some of the results will be given in order to establish a background for a discussion of the convergence of boundary element methods.

Consider the evaluation of the integral

$$\int_1^4 \sqrt{x}\, \mathrm{d}x = \tfrac{14}{3}. \qquad (1)$$

In Figure 1(a) is shown the error of different numerical intergration formulas as a function of the number of function evaluations, M, which is a good measure of the computational work. Note that all curves are straight lines in a double logarithmic co-ordinate system. An analysis of the integration formulas used for Figure 1 reveals that the error E is of the form

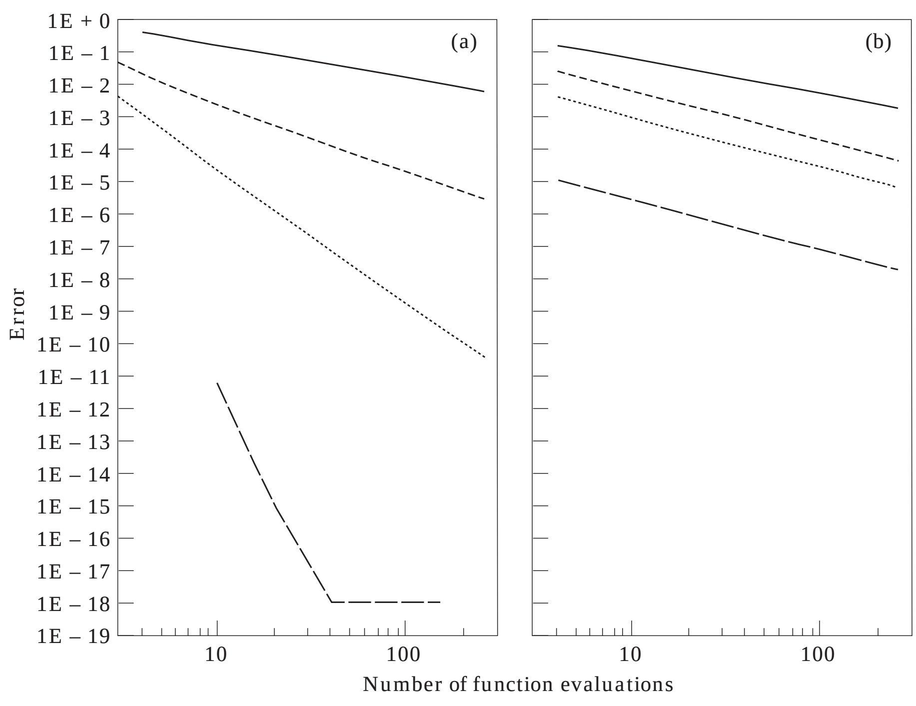

Figure 1. Error as a function of number of function evaluations M for different numerical integration formulas when integrating the square root function: (a) in the interval [1; 4]; (b) in the interval [0, 1]. ——, Left Riemann sum; - - - - , the trapezoidal rule; · · · · · , Simpson's formula; — —; ten-point Gauss–Legendre quadrature.

$$E = \text{const. } M^{-m}, \tag{2}$$

where *const*. is a constant, and m is the order of the integration algorithm. If the function to be integrated is sufficiently smooth (which is the case for equation (1)), m is also the negative value of the slope of the curve obtained when the error is plotted as a function of the number of function evaluations as in Figure 1(a). Hence, a high order method is desired, since it is superior in accuracy to a low order method, and since the accuracy of a high order method improves much faster than that of a low order method as the computational work is increased.

A rough non-mathematical explanation of the numerical integration formulas and their order will be given below. Consider the left Riemann sum. In this formula, the function to be integrated is divided into small segments of equal length h, where $h = 1/M$. In each segment, the function is assumed to be a constant determined by the value of the function at the starting point of the section (the value on the left of each section, hence the name of the formula). Obviously, this formula is able to give an exact value of the integral of a constant function (to the limit of the machine precision), wheras a linear function is not represented exactly by this piecewise constant approximation. Hence, it seems reasonable, and can be shown mathematically, that the error is reduced as h^1, i.e., the order of this formula is one, corresponding to the slope -1 in Figure 1(a). The trapezoidal rule represents the function to be integrated with a piecewise linear approximation. This formula is able to integrate constant and linear functions exactly, whereas a second order variation is not exactly represented by this variation. Hence the order of this formula is $m = 2$, and the slope of the corresponding curve in Figure 1(a) is -2. Simpson's formula is based on a piecewise quadratic interpolation in each segment. For this formula one would expect an order of three, since the third order variation is not represented by this formula. However, due to a cancellation of third order terms, Simpson's formula is of order four corresponding to the slope of -4 in Figure 1(a).

Generally, for these integration formulas, an integration formula based on an intepolation function of order l takes into account $l + 1$ terms of the function's Taylor series, resulting in an integration formula of order $l + 1$.

The final curve in Figure 1(a) shows a formula commonly used for numerical integration, the ten point Gauss–Legendre formula. The order of this formula is 20, but a slope of -20 is not found, since the machine precision is reached after only three subdivisions of the interval.

However, a high order formula does not guaranteee high precision. One of the assumptions of the error analysis is that the function and its derivatives must be sufficiently smooth. As an example of a non-smooth function, consider the integral.

$$\int_0^1 \sqrt{x}\, \mathrm{d}x = \tfrac{2}{3}, \tag{3}$$

in which the first order derivative is singular in $x = 0$. The performance of the numerical integration formulas for this case is shown in Figure 1(b). The left Riemann sum is the only integration formula that exhibits unchanged behaviour; all the higher order formulas now have the same reduced slope of $-1{\cdot}5$ corresponding to the strength of the singularity (of order $\frac{1}{2}$ in the first derivative). This fractional power is not represented in the underlying Taylor series of the formulas, and hence becomes the limiting factor of the convergence. The convergence may be improved/restored by using formulations that are specially designed to deal with the singularity [23]

Hence, a high order formula corresponds to high accuracy only if the function to be integrated is sufficiently smooth. If the function to be integrated or one of its derivatives contains singularities in the interval of interest, these singularities become the limiting factor if the strength of the singularity is larger than the order of the integration formula.

3. THE HELMHOLTZ INTEGRAL EQUATION

To establish a background for discussion of the convergence of boundary element formulations, the method is briefly described in the following.

The direct boundary element method is the numerical solution of the Helmholtz integral equation. The Helmholtz integral equation relates the pressure $p(P)$ outside a vibrating or scattering body to the pressure $p(Q)$ on the surfae of the body, the surface velocity $v(Q)$ normal to the body and (if desired) an incoming wave $p^I(P)$. The formulation used in this paper is a restriction of the general three-dimensional integral equation [2] to axisymmetric geometries and boundary conditions [24, 25] by using a transformation into cylindrical co-ordinates (r, z, θ):

$$C(P)p(P) = \int_L p(Q) \int_0^{2\pi} \frac{\partial G(R)}{\partial n} \,\mathrm{d}\theta \, r_Q \,\mathrm{d}L$$

$$+ \mathrm{i}kz_0 \int_L v(Q) \int_0^{2\pi} G(R) \,\mathrm{d}\theta r_Q \,\mathrm{d}L + 4\pi p^I(P). \quad (4)$$

In this equation, harmonic time variation has been assumed and the time factor $\mathrm{e}^{\mathrm{i}\omega t}$ has been suppressed. This formula is valid in an infinite homogeneous medium (e.g., air) outside an axisymmetric closed body described by its generator L. In the medium p satisfies $\nabla^2 p + k^2 p = 0$. $R = |P - Q|$ is the distance between P and Q. $G(R) = \mathrm{e}^{-\mathrm{i}kR}/R$ is the free-space Green function; $k = \omega/c$ is the wavenumber, where ω is the circular frequency and c is the speed of sound; i is the imaginary unit, z_0 is the characteristic impedance of the medium and n is the unit normal to the surface at the point Q directed away from the body. The quantity $C(P)$ has the value 0 for P inside B and 4π for P outside B. In the case of P on the surface S, $C(P)$ equals the solid angle measured from the medium ($=2\pi$ for a smooth surface).

The term "direct boundary element formulation" refers to the fact that the quantities to be integrated in equation (4) are the physical pressure and normal particle velocity, whereas the term "indirect boundary element formulation" is used for an analogous formula dealing with monopole and/or dipole source distribution(s). In the indirect formulations, the pressure and particle velocity do not appear directly but are related to the density functions of the monopoles and/or dipoles. The density functions of the monopoles and/or dipoles of the indirect formulation are typically found by a variational approach, although a collocation technique is also feasible.

4. NUMERICAL IMPLEMENTATION

As will be briefly described in the following, equation (4) may be solved numerically by assuming that the geometry and the acoustic variables p and v may be described by their values at a finite number M of nodal points. In between the nodes, a continuous variation must be assumed. In this work, two types of variation will be discussed, (i) linear variation and (ii) quadratic variation. Note that the circumferential integrals in equation (4) may be regarded as functions, since they contain no unknown quantities (the unknown pressure or particle velocity has been assumed to be axisymmetric and has been moved outside the circumferential integrals), and therefore equation (4) may be rewritten as

$$C(P)p(P) = \int_L (p(Q)F^B(P, Q) + ikz_0\, v(Q)F^A(P, Q))\, dL + 4\pi p^I(P). \tag{5}$$

Equation (5) is brought to a form suitable for computation by writing the integral on the right side as a sum of integrals each concerning a segment of the generator L_j, where the index $j = 1, 2, \ldots, N$ denotes the number of a segment of the generator. This division must be so fine that two approximations are reasonable (i) the (generally) curved line representing each segment is replaced with a linear or quadratic curve (corresponding to linear or quadratic elements), and (ii) the acoustic variables are assumed to follow a linear or quadratic variation. After these two approximations are made, the geometry of a linear segment can be described by the co-ordinates of the starting point and the end point of each segment—for quadratic interpolation also the mid-point values are needed. The term used for these points is "nodes". Likewise, the values of the acoustic variables are defined by their nodal values. The term used for a segment after these approximations have been carried out is "element", giving the method its name, and the term "shape functions" is often used for the interpolation functions. If the same interpolation function is used for both approximations, the elements are isoparametric, whereas superparametric elements are elements using, for example, a quadratic interpolation for the geometry and linear interpolation for the acoustic variables. If the interpolation function used for the geometry is of higher order than the interpolation function used for the acoustic variables, the elements are subparametric. If one assumes that the normal velocities are known (this is the normal situation), one then has a finite number M of unknown nodal pressures.

In the point collocation approach, the M equations needed to match the M unknowns for finding a unique solution of the problem are then found by placing the point P in turn at M positions (collocation points). Normally, these positions are chosen to be at the nodes on the surface (the so-called surface formulation), since the resulting coefficient matrix becomes dominated by the $C(P)$ terms in the diagonal, which is desirable from a computational point of view. This leaves the problem of handling singular integrals, since the Green function and its normal derivative become singular when R tends to zero; i.e., when the integration point Q passes the calculation point P in the integral on the right side of equation (5). However, this problem is well known and is easily solvable [24]. Alternatively, the calculation point could be placed inside the body, where $C(P) = 0$ (the so-called interior formulation [1]), but this strategy is less desirable, since it does not lead to the desired coefficient matrix with large entries in the diagonal.

Another way of producing the needed M equations is the Galerkin approach. In the Galerkin approach a weighted residual statement is formed by multiplying the residual of the discretized equations with a vector containing the shape functions, integrating over the surface and demanding the result to be zero. The obvious drawback of this method is that an additional integration over the surface of the body is required. In the following, the collocation point method is applied.

Once the problem has been discretized, the resulting equations may be written in matrix form,

$$(\mathbf{C} - \mathbf{D})\mathbf{p} = -ikz_0\, \mathbf{M}\mathbf{v} - 4\pi \mathbf{p}^I, \tag{6}$$

where the complex vector $\mathbf{p}$ contains the nodal pressures, $\mathbf{v}$ contains the nodal normal velocities and $\mathbf{p}^I$ contains the pressure of the incident wave at the nodes in the absence of the body. The matrix **C** is diagonal; its values c_{ii} are the solid angles at node number i. The elements in the matrices **D** and **M** are integrals over the elements of the segments, so that the column number is related to the segment number and row number is the calculation point number. The use of **M** and **D** refers to the fact that they contain integrals over the Green function and its derivative, respectively. These terms are often interpreted as the monopole term and the dipole term.

5. CONVERGENCE OF THE BOUNDARY ELEMENT METHOD

For the boundary element formulation described in the previous section, five sources of errors may be identified: (i) uncertainties in calculating the functions F^A and F^B in equation (5), (ii) approximations of the boundary, (iii) aproximations of the acoustic variables, (iv) the numerical integration over each element and (v) errors in the solution of the system of equations.

In the following, it will be assumed that the error in determining the functions F^A and F^B is negligible. This assumption seems allowable if the singular integrals mentioned in the previous section are correctly handled. Moreover, it is possible to test the validity of this assumption at a later stage.

It will also be assumed that the error due to numerical integration is negligible, and it turns out that this criterion can be used to decide the minimum order of the numerical integration formula [7] depending on the order 2β of the elliptic operator. For the Helmholtz integral equation, $2\beta = 0$ [5, 7], and the order of integration must be at least one-half more than the order to the error due to discretization. Numerical experiments confirmed that for qudratic elements a four-point Gauss–Legendre quadrature formula gave the same accuracy and convergence rate as all higher order quadrature formulas, whereas a two-point Gauss–Legendre quadrature formula destroyed the accuracy and convergence rate, in agreement with the theory in reference [7] (the three-point formula has not been used, since one of the integration points then coincides with the singularity).

Finally, it will be assumed that the error in solving the system of equations is negligible. This is more disputable since it is a well-known fact [1, 26] that the system of equations is ill-conditioned at or near the so-called characteristic frequencies, and that the solution then may be wrong. However, for the geometries considered here, the characteristic frequencies are known in advance and have been avoided, and it has been found that for all cases the resulting system of equations is well-conditioned. A favourable feature of the surface formulation considered here is that the condition number of the resulting coefficient matrix tend to a constant as the number of elements is increased [7], so the set of equations does not become more ill-conditioned in the limit of $h \to 0$ as is the case in some other numerical schemes. Furthermore, in reference [7] it was found that the convergence rate was not destroyed even when very close to the characteristic frequencies (although the level of error was dramatically increased). Only exactly at a characteristic frequency (up to six significant digits) the formulation failed to converge. A similar experiment (not shown here) carried out on the present formulation showed the same behaviour.

Hence, the present work deals with the errors due to the discretization of the geometry and of the acoustic variables. Initially, only the error due to the approximation of the acoustic variables is considered here. The effect of discretizing the geometry is considered later.

Consider the solution of a scattering problem in which the body is infinitely hard (i.e., $\mathbf{v} = \mathbf{0}$) and smooth (i.e., $C(P) = 2\pi$ for all collocation points P). If it is assumed that the dipole matrix is the sum of an exact part $\bar{\mathbf{D}}$ and a part $\tilde{\mathbf{D}}$ that contains the error due to the discretization of the pressure, equation (6) may be written as

$$(\mathbf{C} - \bar{\mathbf{D}} - \tilde{\mathbf{D}}) \cdot (\bar{\mathbf{p}} + \tilde{\mathbf{p}}) = \mathbf{p}^I, \tag{7}$$

where the tilde denotes the error made by the approximation and the bar denotes the true vectors or matrices. Likewise, it is assumed that the pressure may be written as a sum of an exact part and a resulting error. Note that the right side is given with no errors. By working out the left side of equation (7) and using $(\mathbf{C} - \bar{\mathbf{D}})\bar{\mathbf{p}} = \mathbf{p}^I$, the equation

$$(\mathbf{C} - \bar{\mathbf{D}})\tilde{\mathbf{p}} = \tilde{\mathbf{D}}(\bar{\mathbf{p}} + \tilde{\mathbf{p}}) \tag{8}$$

is found. If one assumes that making the mesh finer reduces the error (i.e., if one assumes that the method converges which is proven in reference [5]), then $\tilde{\mathbf{p}}$ will become much smaller than $\bar{\mathbf{p}}$ as $M \to \infty$, and equation (8) then reduces to

$$(\mathbf{C} - \bar{\mathbf{D}})\tilde{\mathbf{p}} = \tilde{\mathbf{D}}\bar{\mathbf{p}}. \tag{9}$$

Note that this analysis concerns the effect of discretization of the acoustic variables only—the discretization with respect to the geometry is treated later in this paper (and theoretically in references [5, 7]). Suppose that the object is divided into linear or quadratic elements of the same size. For convenience of the following analysis, each element is transformed into a standard interval $[0; h]$. (In an actual implementation the parent element interval is normally $[-1; 1]$, but if this interval is used the analysis below would then be a bit more tedious and would give the same result.) The elements of $\mathbf{D} = \bar{\mathbf{D}} + \tilde{\mathbf{D}}$ can then be written in the form

$$\int_0^h N_\alpha(x) F^B(P, Q(x)) J(x)\, \mathrm{d}x, \tag{10}$$

where $J(x)$ is the Jacobean of the transformation, and the N_α's are the shape functions. If it is assumed that the pressure and its derivatives are sufficiently smooth, the exact value of the pressure p in an element will be given as

$$p(x) = \sum_{\alpha=1}^{m} p_\alpha N_\alpha(x) + h^m \frac{\partial^m p(x_0)}{\partial x^m} \frac{1}{m!}, \tag{11}$$

according to Taylor's formula. Here x_0 is an unknown point between 0 and h. Hence the elements in $\tilde{\mathbf{D}}$ are of the form

$$\int_0^h h^m \frac{\partial^m p(x_0)}{\partial x^m} \frac{1}{m!} F^B(P, Q(x)) J(x)\, \mathrm{d}x. \tag{12}$$

By the use of partial integration it can now be seen that in the limit of small element length h the elements in $\tilde{\mathbf{D}}$ are proportional to h^{m+1}. Note that the dimension M of $\tilde{\mathbf{D}}$ is inversely proportional to h. Hence, each element in the vector $\tilde{\mathbf{D}}\bar{\mathbf{p}}$ is the sum of $M \propto 1/h$ terms of magnitude h^{m+1}, and therefore of the magnitude h^m, since the true solution $\bar{\mathbf{p}}$ is slowly varying in the limit of small h. Now, consider the left side of equation (9). The elements in a single row of the matrix $\bar{\mathbf{D}}$ are related to a surface integral over the object, since each element in $\bar{\mathbf{D}}\bar{\mathbf{p}} = C(P)p_{true}(P)$ is the value of the surface integral of the true pressure times the derivative of the Green function with respect to the collocation point P. This integral is in the limit a constant (the solid angle 2π times the true pressure at P), and therefore each element in the matrix $\bar{\mathbf{D}}$ is of magnitude h (i.e., the magnitude of each element

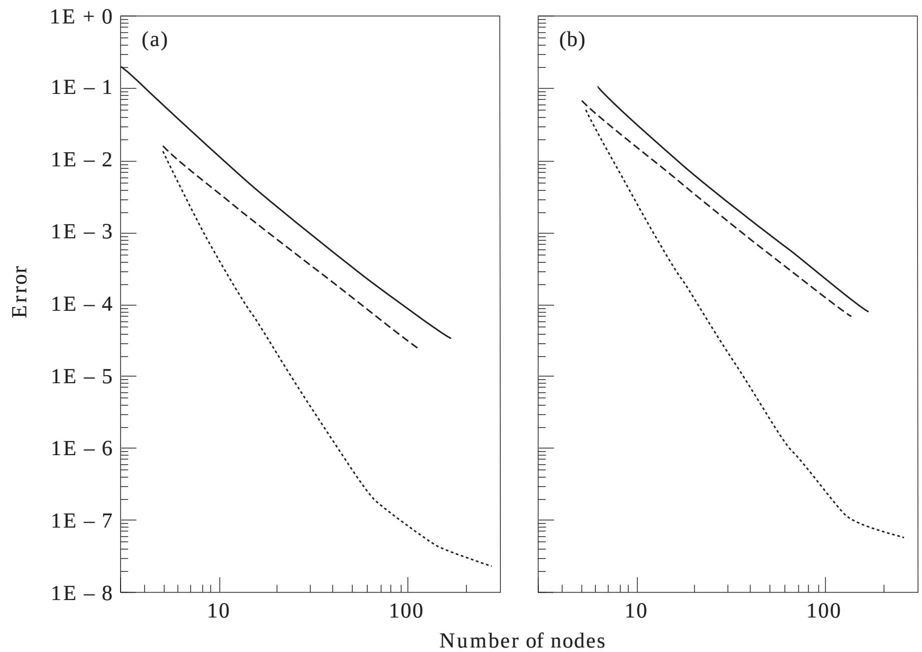

Figure 2. Error as a function of number of nodes M for different boundary element formulation applied to the problem of scattering by a rigid sphere: (a) $ka = 1$; (b) $ka = 2$. ——, Isoparametric linear formulation; - - - - , superparametric linear/quadratic formulation; · · · · , isoparametric quadratic formulation.

decreases proportional to the length of the integration interval, which seems reasonable). Now, *suppose* that the elements in $\tilde{\mathbf{p}}$ are of order m_1 (i.e., of magnitude h^{m_1}). Then each element of $\bar{\mathbf{D}}\tilde{\mathbf{p}}$ must also be of magnitude m_1 since each element of $\bar{\mathbf{D}}\tilde{\mathbf{p}}$ is a sum of $M \propto 1/h$ terms of magnitude $hh^{m_1} = h^{m_1+1}$. Likewise, $\mathbf{C}\tilde{\mathbf{p}} = 2\pi\tilde{\mathbf{p}}$ is of magnitude m_1. Hence, the right side of equation (9) is of the same magnitude as $\tilde{\mathbf{p}}$, m_1, and since the left side of equation (9) is of magnitude m, $m_1 = m$ is found.

For linear shape functions the expected convergence rate $m = 2$ is found, and for quadratic shape functions the expected convergence rate is $m = 3$. Hence, the result of this loose study is consistent with the findings of the mathematical sound study of others [5, 7].

5.1. SCATTERING BY A RIGID SPHERE

The first test case concerns scattering of a plane wave by a rigid sphere. For this case, an analytical solution is known. The errors E shown in Figure 2 are calculated as the ratio of the length of the residual vector and the length of the analytical solution

$$E = \frac{\|\mathbf{r}\|_2}{\|\mathbf{p}_{ana}\|_2} = \sqrt{\frac{\sum_{i=1}^{M}((\mathrm{Re}\{p_{ana}[i]\} - \mathrm{Re}\{p_{bem}[i]\})^2 + (\mathrm{Im}\{p_{ana}[i]\} - \mathrm{Im}\{p_{bem}[i]\})^2)}{\sum_{i=1}^{i=M}((\mathrm{Re}\{p_{ana}[i]\})^2 + (\mathrm{Im}\,p_{ana}[i]\})^2)}}. \quad (13)$$

Note that this measure of error ensures that if the error on each element is of order m, then the total error E is of the same order. In Figure 2 are shown the errors made by three different boundary element formulations at two frequencies corresponding to $ka = 1$

(Figure 2(a)) and $ka = 2$ (Figure 2(b)) as functions of the number of nodes M. The nodes are placed with equal spacing on the generator of the sphere. (A number of frequencies have been tested and the results showed the same qualitative behaviour.) It can be seen that all curves are roughly straight lines in a double logarithmic co-ordinate system, which means that the error is of the form described by equation (2). It is also shown in Figure 2 that the error at the higher frequency is larger than at the lower frequency for the same discretization, and that the rate of convergence is the same for the same formulation at the two frequencies. Hence, the dependence of frequency of the error is reflected in a vertical displacement of the curves in Figure 2. The solid lines in Figure 2 represent the isoparametric linear formulation. They both have a slope around -2, corresponding to an order of two, which is consistent with the theory presented in the last section. The dashed curves represent a superparametric formulation using linear interpolation for the pressure and quadratic interpolation for the geometry. In this formulation, the approximation with regard to the geometry should soon become insignificant compared to the approximation on the pressure as the number of nodes is increased. It can be seen that the curves representing the superparametric formulation are parallel to the curves representing the isoparametric linear formulation. Thus these two formulations are of same order. If the error due to the geometric discretization of the isoparametric linear formulation were of *higher* order than the error due to the discretization of the pressure, both the isoparametric and superparametric would be dominated by errors due to discretization of the pressure at high values of M, and the curves would coincide. On the other hand, if the error due to the geometric discretization of the isoparametric linear formulation were of *lower* order than the error due to the discretization of the pressure, this error would dominate in the isoparametric formulation, and the two curves would have different slope. Consequently, the error due to geometric discretization must be of the same order as the error due to discretization of the pressure for the isoparametric linear formulation, in agreement with references [5, 7].

The dotted curves in Figure 2 represent the isoparametric quadratic formulation. It can be seen that the slope of these curves is about -4, corresponding to an order of four. Hence, it seems that the third order terms one would expect from the theory in the last section cancel out in the same manner as in Simpson's formula, discussed in section 2. An analogous result of "superconvergence" for constant elements was found in reference [7]. It can also be seen that about $E = 1\mathrm{E} - 7$ the curve flattens (which was also the case for the Gaussian quadrature formula in Figure 1(a)). The reason for this is believed to be the limited precision of the evaluation of the F^B terms of equation (5).

5.2. GEOMETRIC SINGULARITIES

Another way of studying the error due to the discretization of the acoustic variables is to choose a geometry that is exactly described. In an axisymmetric formulation a cylinder consists of three linear segments describing the generator, and the geometry is exactly described at all levels of discretization. Scattering by a rigid cylinder was studied by using the isoparametric linear and quadratic formulations (the results of the superparametric formulation coincide with the result of the linear formulation). In Figure 3 is shown the error of the linear and quadratic formulations at the frequency corresponding to $ka = 1$ as a function of the number of nodes M. In each test case, the nodes are equally spaced on the generator. Since an analytical solution is not available for this test case, a very finely meshed boundary element calculation was used as reference. It was assured that the accuracy of the reference solution was much higher than of the calculations shown. The most noticeable feature of Figure 3 is that the two formulations have the same slope of about $-1{\cdot}2$, which is very far from the value of four that was expected for the quadratic formulation. The reason for this behaviour is the geometric singularities (the edges) of the cylinder, which cause a degradation of the rate of convergence analogous to the case of regular numerical integration of a function with singularities described in section 2 (see Figure 1(b)).

The asymptotic behaviour of the pressure near an edge may be found by the following loose study (for a more rigid development the reader should refer to reference [27, see p. 187]). Consider the sound field near the edge of the cylinder. For the diffraction problem, the term of interest is kr, where r is the distance from the edge. Now, for any finite frequency, kr tends to zero when r tends to zero, but since the diffraction problem is governed by kr it is mathematically legitimate to keep r constant and let k tend to zero instead, and still draw the same conclusions from the approximate study. Hence, in the limit of $r \ll 1/k$, Laplace's equation may be used. For Laplace's equation, traditionally used in the limit of small k, it is well known that an edge of angle $3\pi/2$ produces an $r^{-1/3}$ behaviour of the flow velocity at the edge—the general rule is that an angle α produces an $r^{\pi/\alpha - 1}$ behaviour of the flow velocity [28, p. 69]. Hence, the particle velocity tends to infinity as r tends to zero. The well-known $r^{-1/2}$ behaviour of the particle velocity near the edge of a thin screen [27, p 505, 12–15] may also be explained in this way. Hence the pressure near the edge of the cylinder shows an $r^{2/3}$ behaviour that is taken into account neither by the linear nor the quadratic formulation and therefore becomes the limiting factor on the rate of convergence.

5.3. SINGULAR INTERPOLATION FUNCTIONS

For linear elements, each segment is normally transformed into the interval $[-1, 1]$, and in each segment the pressure is approximated by linear functions:

$$p(x) = p_{-1}\,\mathbf{\Psi}_{-1}(x) + p_{+1}\,\mathbf{\Psi}_{+1}(x), \tag{14}$$

where

$$\mathbf{\Psi}_{-1}(x) = \tfrac{1}{2}(1 - x), \qquad \mathbf{\Psi}_{+1}(x) = \tfrac{1}{2}(1 + x), \qquad x \in [-1, 1], \tag{15}$$

and p_{-1} and p_{+1} are the nodal values of the left and right sides of the element respectively. These linear interpolation functions are a development from the set $\{1, x\}$, and are found by the requirements $p(-1) = p_{-1}$ and $p(1) = p_{+1}$.

Consider the case of an $r^{2/3}$ singularity on the right side ($x = +1$) of the transformed interval. The singular interpolation functions $\mathbf{\Phi}$ must be developed from the functions $\{1, (1 - x)^{2/3}\}$ in order to represent a constant value and a variation corresponding to the singularity. Hence $\mathbf{\Phi}_{-1}$ and $\mathbf{\Phi}_{+1}$ are of the form

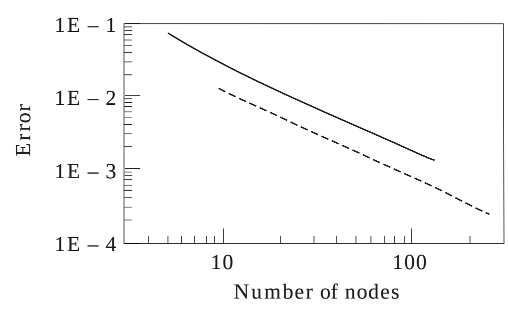

Figure 3. Error as a function of number of nodes M for different boundary element formulation applied to the problem of scattering by a rigid cylinder. ——, Isoparametric linear formulation; - - - - -, isoparametric quadratic formulation.

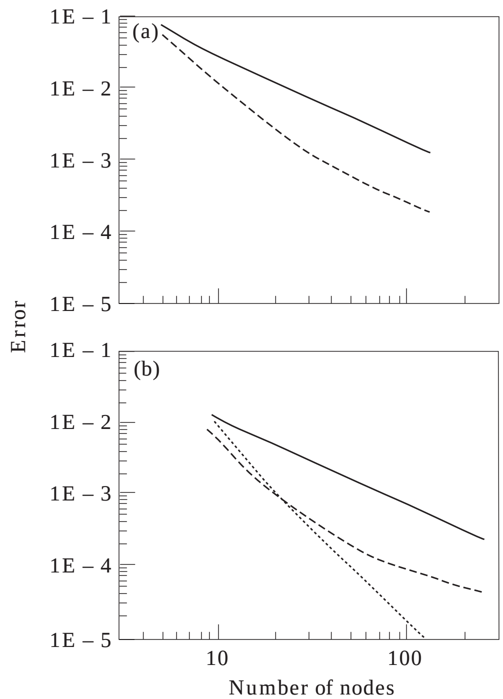

Figure 4. Error as a function of number of nodes M for different boundary element formulation applied to the problem of scattering by a rigid cylinder. (a) ——, Isoparametric linear formulation; - - - - - - , specialized linear formulation. (b) ——, Isoparametric quadratic formulation; - - - - - , isoparametric quadratic formulation with the generalized quarter point formulation; · · · · , isoparametric quadratic formulation with singular shape functions.

$$\mathbf{\Phi} = \alpha_1 + \alpha_2 (1 - x)^{2/3}. \tag{16}$$

The constants α may be found by the requirements $\mathbf{\Phi}_{-1}(-1) = 1$, $\mathbf{\Phi}_{-1}(1) = 0$ and $\mathbf{\Phi}_{+1}(-1) = 0$, $\mathbf{\Phi}_{+1}(1) = 1$, which yield

$$\mathbf{\Phi}_{-1} = 2^{-2/3}(1 - x)^{2/3}, \qquad \mathbf{\Phi}_{+1} = 1 - 2^{-2/3}(1 - x)^{2/3}. \tag{17a, b}$$

Similarly, interpolation functions may be found for the case of a singularity on the left ($x = -1$) of the interval.

In Figure 4(a) is shown the error of the original linear formulation and the improved formulation as a function of the number of nodes. For rough meshes (i.e., meshes with few nodes) the original order of two of the linear formulation is restored, but for fine meshes the slope is gradually reduced to $-1{\cdot}2$. This reduction of the slope for finer meshes is believed to be due to the fact that as the mesh is refined the element next to the singular element gets close to the singularity and exhibits a singular behaviour. It should be noted that the accuracy at the stage when the improved formulation reduces its slope is sufficient for most practical purposes.

5.4. GENERALIZED QUARTER POINT TECHNIQUE

Wu and Wan [13, 14] have adopted the so-called quarter point technique from the finite element method to model the $r^{1/2}$ singularity that arises at the edge of a thin screen (knife edge singularity). It can be shown that if the mid-element node of an isoparametric quadratic element is moved from the middle to a position of one-fourth of an element length to the singularity, the quadratic element exactly models the square root function (i.e., the element represents a development from the set $\{1, x^{1/2}, x\}$). Note that for a normal element the mid-element node cannot be chosen freely—it should be in the geometric mid-point of the element in order to model a quadratic variation. Hence, it can be said that this technique violates the element (by performing an illegal movement of the mid-element node) in such a way that instead of modelling a second order variation, a variation corresponding to the singularity is modelled.

The idea that now arises is a generalization of the quarter point technique. By trial and error, the mid-element node of an isoparametric quadratic element has been moved towards the position of the singularity of the $r^{2/3}$ function, and it was found that at a distance of 0·275 times the element length from the singularity the $r^{2/3}$ function was well modelled. In Figure 5(a) it is shown how the $r^{2/3}$ function is modelled with a normal quadratic element, and in Figure 5(b) it is shown how the function is modelled using the generalized quarter point technique. It is evident that the function is not modelled exactly by using this approach as is the case for the square root singularity and the quarter point technique, but the modelling is still very good. Since using the generalized quarter point technique corresponds to an expansion from the set $\{1, (1-x)^{2/3}, x\}$, the $\tilde{\mathbf{D}}$ matrix will contain a fixed number of terms that are proportional to h^3 in each row (since the first term not modelled is of order h^2 and the matrix contains the integral of this term). Hence the expected slope of this formulation will be minus three. In Figure 5(b) is shown the error of the original quadratic formulation, and the error of the generalized quarter point formulation compared to the error of a specialized formulation in which singular shape functions is applied. For the generalized quarter point formulation an initial slope of about -3 is found, but for finer meshes the slope decreases to the value of $-1{\cdot}2$ of the original formulation. This is believed to be due to the fact that the singularity is only approximately modelled by the generalized quarter point technique. Hence, it appears that for rough meshes the singular behaviour is adequately modelled by the generalized quarter point technique, whereas for fine meshes it is not. The curve representing the specialized formulation using singular elements is slightly curved. This is believed to be due to nearly singular behaviour of the elements next to the elements containing the singularity for fine meshes as it also seemed to be the case for linear elements. For rough meshes the generalized quarter point technique performs slightly better than the specialized

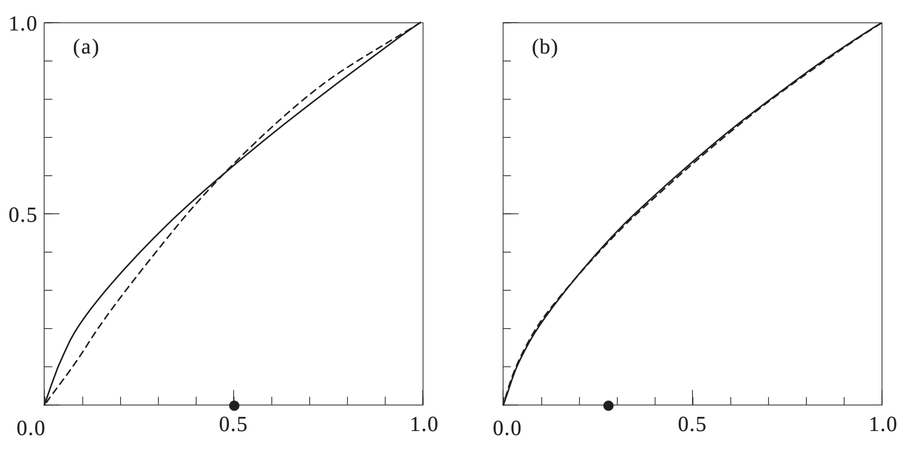

Figure 5. Modelling of the $r^{2/3}$ function: (a) using normal isoparametric quadratic elements; (b) using the generalized quarter point formulation. The placement of the mid-element node is indicated with a bold dot on the r-axis.

formulation using singular shape functions whereas the contrary is the case for fine meshes. Hence, a crossover exists for which the specialized formulation is more advantageous than the generalized quarter point technique. For the test case shown here, this crossover is below an accuracy of 0·001 (less than 0·01 dB), so the generalized quarter point technique is preferable for most practical purposes. Test cases involving other frequencies all showed similar behaviour.

6. DISCUSSION

The test cases presented are rather academic, since the geometries are simple and since elements of the same size have been used. For practical purposes involving more complex geometries, equally sized elements would not be feasible, and closer spacing between the elements would be used where the user expects the variation of the acoustic variables to be strong. However, for a complex problem the qualitative behaviour of the solution error found in these simple cases is still expected as the mesh is refined.

Edges generally give rise to singularities in one of the derivatives of the pressure. Note that for angles larger than π the first derivative of the pressure (i.e., the particle velocity) tends to infinity; for angles between $\pi/2$ and π the second derivative of the pressure tends to infinity; for angles between $\pi/3$ and $\pi/2$ the third derivative of the pressure tends to infinity, etc. The need for modelling these higher order singularities depends on the order of the formulation used. When using a linear formulation all singularities in the first order derivative of the pressure should be modelled, since they would destroy the order of two of the linear formulation, whereas a quadratic formulation requires all singularities up to the third derivative of the pressure to be modelled, if the high order of four of this formulation is to be retained. It is also interesting to note that edges corresponding to an integer fraction of π ($\pi/2$, $\pi/3$, . . .) do not give rise to singularities, and that exactly these values correspond to the problems in which image source modelling is feasible.

The most obvious way of modelling a singularity would be to use a standard formulation with a graded mesh near the singularity [17]. Two drawbacks are connected with this approach. First of all, the method is inefficient since unneeded nodes must be introduced and, second, it is desirable that all elements of the model are of approximately the same size, since the resulting set of equations otherwise could become ill-conditioned.

Of the two methods examined here to model the singularity, the author favours the generalized quarter point technique, since it may be realized by changing the input to the BEM code, whereas the technique using specialized shape functions requires the BEM code itself to be changed.

7. CONCLUSIONS

In this paper a discussion has been presented of convergence of boundary element formulations. Convergence of boundary element methods has been discussed in a number of journals in the areas of mathematics, numerical analysis and computational physics. Results from these papers that are relevant for the present study have been compiled and presented in the present paper.

As an alternative to the somewhat complicated theory of convergence developed in the mathematical literature, a simple, intuitive and non-mathematical convergence analysis has been carried out. The results of this analysis agree with the results of the rigid mathematical analysis and with the numerical experiments.

The order of both the isoparametric and superparametric linear fomulation is found to be two, whereas the order of the isoparametric quadratic formulation is four. The influence of frequency on the accuracy of a boundary element calculation is generally that higher frequency gives rise to larger error for the same mesh, but the rate of convergence is unaffected by the frequency.

Bodies with edges give rise to geometric singularities that reduce the rate of convergence of the formulations. Two methods that overcome this difficulty are examined. One of these applies specialized shape functions to deal with the geometric singularity, whereas the other models the singularity by a displacement of the mid-element node in a quadratic element. The latter approach may readily be used with existing codes, and has been named the generalized quarter point technique. These two specialized formulations improve the accuracy considerably and restore a high order of convergence for the rough meshes that are usually applied for engineering purposes.

REFERENCES

1. H. A. Schenck 1968 *Journal of the Acoustical Society of America* **44**, 41–58. Improved integral formulation for acoustic radiation problems.
2. A. F. Seybert, B. Soenarko, F. J. Rizzo and D. J. Shippy 1986 *Journal of the Acoustical Society of America* **77**, 362–368. An advanced computational method for radiation and scattering of acoustic waves in three dimensions.
3. J. J. Engblom and R. B. Nelson 1975 *Journal of Applied Mechanics—Transactions of the ASME*, *ASME paper no*. 75-*AMPW*-54, 295–300. Consistent formulation of sound radiation from arbitrary structure.
4. R. D. Ciskowski and C. A. Brebbia (editors) 1991 *Boundary Element Methods in Acoustics*. Southampton: Computational Mechanics Publications.
5. W. L. Wendland 1983 in *Theoretical Acoustics and Numerical Techniques* (P. Filippi, editor). CISM Courses and Lectures no. 277. Wien–New York: Springer-Verlag. Boundary element methods and their asymptotic convergence.
6. E. P. Stephan 1988 in *Boundary Elements X Vol*. 1: *Mathematical and Computational Aspects* (C. A. Brebbia, editor), 205–216. Southampton: Computational Mechanics Publications. The H-P version of the Galerkin boundary element method for integral equations on polygons and open arcs.
7. S. Amini and S. M. Kirkup 1995 *Journal of Computational Physics* **118**, 208–221. Solution of Helmholtz equation in the exterior domain by elementary boundary integral methods.
8. A. J. Burton and G. F. Miller 1971 *Proceedings of the Royal Society of London* **A323**, 201–210. The application of integral equation methods to the numerical solutions of some exterior boundary value problems.
9. J. J. Grannell, J. J. Shirron and L. S. Couchman 1994 *Journal of the Acoustical Society of America* **95**, 2320–2329. A hierarchic *p*-version boundary-element method for axisymmetric acoustic scattering and radiation.
10. P. Geng, J. T. Oden and L. Demkowicz 1996 *Journal of the Acoustical Society of America* **100**, 335–345. Numerical solution and *a posteriori* error estimation of exterior acoustics problems by a boundary element method at high wave numbers.
11. P. J. T. Filippi 1988 in *Boundary Elements X Vol* 4: *Geomechanics*, *Wave Propagation and Vibrations* (C. A. Brebbia, editor), 269–287. Springer-Verlag. Boundary element methods in acoustics and vibrations: a review of the last twenty years.
12. A. F. Seybert, Z. H. Jia and T. W. Wu 1992 *Journal of the Acoustical Society of America* **91**, 1278–1283. Solving knife-edge scattering problems using singular boundary elements.
13. T. W. Wu and G. C. Wan 1992 *Journal of the Acoustical Society of America* **92**, 2900–2906. Numerical modelling of acoustic radiation and scattering from thin bodies using a Cauchy principal integral equation.
14. T. W. Wu and G. C. Wan 1992 *Proceedings*. *Second International Congress on Recent Developments in Air- and Structure-Borne Sound and Vibration* (M. J. Crocker and P. K. Raju, editors), 993–999. Isoparametric boundary element modeling of acoustical cracks.
15. K.-D. Ih and D.-J. Lee 1997 *Journal of Sound and Vibration* **202**, 361–373. Development of the direct boundary element method for thin bodies with general boundary conditions.
16. D. Henshell 1975 *International Journal for Numerical Methods in Engineering* **9**, 495–507. Crack tip finite elements are unnecessary.

17. V. J. ERVIN and E. P. STEPHAN 1987 in *Boundary Elements IX Vol*. 1: *Mathematical and Computational Aspects* (C. A. Brebbia, W. L. Wendland and G. Kuhn, editors), 167–175. Southampton: Computational Mechanics Publications. Experimental convergence of boundary element methods for the capacity of the electrified square plate.
18. E. RANK 1987 in *Boundary Elements IX Vol*. 1: *Mathematical and Computational Aspects* (C. A. Brebbia, W. L. Wendland and G. Kuhn, editors), 259–278. Southampton: Computational Mechanics Publications. Adaptive boundary element methods.
19. E. P. STEPHAN 1996 *Computer Methods in Applied Mechanics and Engineering* **133**, 183–208. The *h-p* boundary element for solving 2- and 3-dimensional problems.
20. H. HOLM, M. MAISCHAK and E. P. STEPHAN 1996 *Computing* **57**, 105–134. The hp-version of the boundary element method for Helmholtz screen problems.
21. S. M. KIRKUP and D. J. HENWOOD 1994 *Applied Mathematical Modelling*, 32–38. An empirical error analysis of the boundary element method applied to Laplace's equation.
22. W. H. PRESS, B. P. FLANNERY, S. A. TEUKOLSKY and W. T. VETTERLING 1986 *Numerical Recipes*. Cambridge: Cambridge University Press.
23. A. H. STROUD and D. SECREST 1966 *Gaussian Quadrature Formulas*. Englewood Cliffs, New Jersey: Prentice-Hall.
24. A. F. SEYBERT, B. SOENARKO, F. J. RIZZO and D. J. SHIPPY 1986 *Journal of the Acoustical Society of America* **80**, 1241–1247. A special integral equation formulation for acoustic radiation and scattering for axisymmetric bodies and boundary conditions.
25. P. JUHL 1993 *Journal of Sound and Vibration* **163**, 397–406. An axisymmetric integral equation formulation for free space non-axisymmetric radiation and scattering of a known incident wave.
26. P. JUHL 1994 *Journal of Sound and Vibration* **175**, 39–50. A numerical study of the coefficient matrix of the boundary element method near characteristic frequencies.
27. A. D. PIERCE 1989 *Acoustics*: *An Introduction to its Physical Principles and Applications*. Woodbury, New York: The Acoustical Society of America; second edition.
28. H. LAMB 1932 *Hydrodynamics*. New York: Dover (1945); sixth edition.